

# Effective Design of Graphene Patch Arrays for Adjustable Plane-Wave Scattering

Stamatios Amanatiadis

Dept. of Electrical & Comp. Eng.  
Aristotle University of Thessaloniki  
Thessaloniki, Greece  
samanati@auth.gr

Tadao Ohtani

1-17-134 Omachi  
Asahikawa, Japan  
bytcg100@ybb.ne.jp

Yasushi Kanai

Department of Engineering  
Niigata Institute of Technology  
Kashiwazaki, Japan  
kanai@iee.niit.ac.jp

Nikolaos Kantartzis

Dept. of Electrical & Comp. Eng.  
Aristotle University of Thessaloniki  
Thessaloniki, Greece  
kant@ece.auth.gr

**Abstract**—In this paper, the scattering properties of graphene patches are investigated to design arrays that are able to control effectively plane wave propagation. Initially, single patches are examined in terms of their radar cross-section and surface wave generation. Moreover, an array of four identical elements is designed and thoroughly investigated indicating that electrostatic bias field has not a significant effect. However, the application of non-uniform biasing on the same setup reveals the fine adjustment of the scattered wave’s main lobe direction.

**Index Terms**—anisotropy, beam manipulation, chemical potential, surface waves.

## I. INTRODUCTION

Recently, technological advancements require efficiently adjustable devices such as radiators with beam manipulation features [1]. Moreover, the operation frequencies are continuously increasing, approximating THz regime, to support the demands of data rate transfer. However, conventional materials, such as metals, present degraded performance at this spectrum resulting in the consideration of alternative ones, such as the popular graphene [2]. Despite its negligible thickness, this truly two-dimensional carbon allotrope has gained significant recognition due to its exotic properties, such as the ability to support strongly confined surface plasmon polariton (SPP) waves at far-infrared frequencies.

This feature is exploited in this work to control the scattering properties of a graphene patch with finite dimensions. Specifically, our initial goal is the radar cross-section extraction of single square patches as well as the observation of surface wave generation onto graphene that are strongly connected to the application of electrostatic bias fields. To this end, the two-dimensional material is introduced in a properly modified Finite-Difference Time-Domain scheme as an equivalent surface current density that depends on graphene’s surface conductivity [3]. Then, a  $2 \times 2$  patch array setup is examined indicating that a non-uniform electrostatic biasing is able to rotate finely the main-lobes of both back and forward scattered waves.

## II. GRAPHENE CONDUCTIVITY AND SURFACE WAVES

In our work, graphene is considered as infinitesimally thin layer, characterized via its surface conductivity  $\sigma(\omega, \mu_c, \Gamma, T)$ ; where  $\omega$  is the radian frequency,  $\mu_c$  the chemical potential

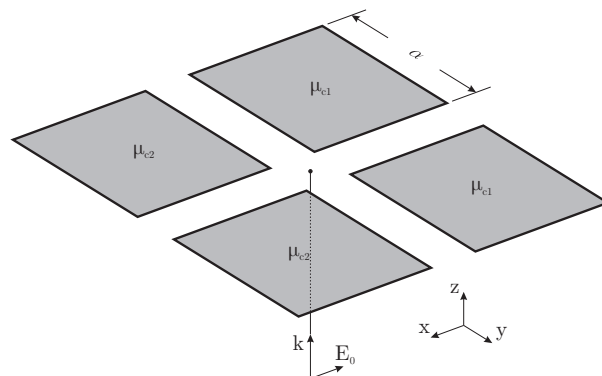


Fig. 1. Plane wave propagating towards a  $2 \times 2$  graphene patch array.

that is controlled via an applied electrostatic bias,  $\Gamma$  a phenomenological scattering rate assumed to be independent of energy, and  $T$  the temperature. Graphene’s conductivity is evaluated by the compact expression resulting from the Kubo formula [4], involving only the dominant, at the far-infrared spectrum, intraband term:

$$\sigma_{\text{intra}}(\omega, \mu_c, \Gamma, T) = \frac{e^2 k_B T}{\pi \hbar^2 (j\omega + 2\Gamma)} \times \left[ \frac{\mu_c}{k_B T} + 2 \ln(e^{-\mu_c/k_B T} + 1) \right]. \quad (1)$$

Moreover, the propagation properties of the surface wave onto graphene are evaluated via the complex wavenumber  $k_\rho$  of that depends on the material’s conductivity and is extracted via [5]:

$$k_\rho = k_0 \sqrt{1 - \left( \frac{2}{\sigma_{\text{intra}} \eta_0} \right)^2}, \quad (2)$$

with  $k_0$  and  $\eta_0$  the free space wavenumber and wave impedance, respectively. An additional, more intuitive feature of the SPP wave is its wavelength  $\lambda_{SPP}$  that is promptly calculated in terms of:

$$\lambda_{SPP} = \frac{2\pi}{\Re\{k_\rho\}}. \quad (3)$$

## III. PLANE WAVE SCATTERING ON GRAPHENE PATCHES

The general setup that is under investigation is depicted in Fig. 1, where graphene is on  $xy$ -plane and a plane wave is

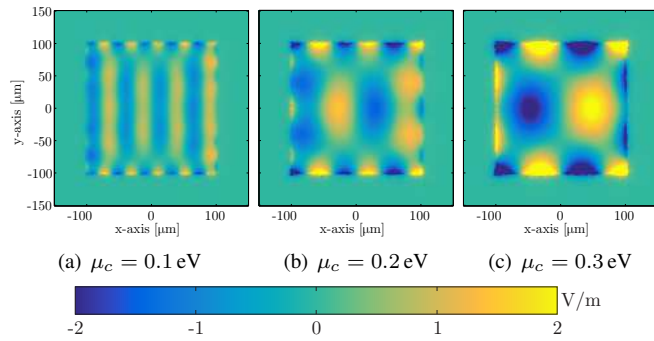


Fig. 2. Distribution of electric field component that is normal to graphene.

propagating towards positive  $z$ -axis, that is normal to graphene surface. Observe that the plane wave polarization is along negative  $x$ -axis. The computational domain for the subsequent analyses is divided into  $300 \times 300 \times 300$  cells with  $\Delta x = \Delta y = \Delta z = 2.5 \mu\text{m}$  and a time-step of  $\Delta t = 4.5 \text{fs}$ , while open boundaries are terminated with an 8-cell perfectly matched layer. The simulations are conducting at operating frequency 1–2 THz, where graphene SPP wave contribution is enhanced, while the dimension of square patches is selected  $\alpha = 100 \mu\text{m}$ . Finally, graphene parameters are set to  $\Gamma = 0.33 \text{meV}$  and the chemical potential varies from low to moderate values, specifically 0.1 – 0.3 eV.

#### A. Single Patch Scenario

Initially, a single graphene patch is placed into the computational domain and the generation of surface waves is investigated thoroughly. In particular, the distribution of the normal, to graphene, electric field component, namely  $E_z$ , is depicted in Fig. 2 for different chemical potential values. It is evident that as the latter increases, the SPP wavelength is larger, as expected through (3), where  $\lambda_{SPP}$  is 26.3, 50 and  $70.2 \mu\text{m}$  for  $\mu_c$  equal to 0.1, 0.2 and 0.3 eV, accordingly. Moreover, the standing waves are appearing towards polarization, while electric field is stronger as chemical potential increases that can be explained due to the weaker matching of the propagating surface wave to the surface waves with decreased wavelength. Finally, the directivity of the scattered wave is evaluated and sketched in Fig. 3. It is evident that resonance regions exist due to the surface wave stimulation, while chemical potential variation is able to influence the resonance frequency.

#### B. Array of Graphene Patches

In our second scenario, the  $2 \times 2$  array of Fig. 1 is investigated at 1.8 THz, where the resonance frequency of  $\mu_c = 0.3 \text{eV}$  patch is observed. Firstly, graphene patches are uniformly biased with  $\mu_{c1} = \mu_{c2} = 0.1 \text{eV}$  while a final setup is designed, where the patches are distinguished in two groups along the polarization. Two different cases are examined, the former with  $\mu_{c1} = 0.1 \text{eV}$  and  $\mu_{c2} = 0.2 \text{eV}$ , the latter with  $\mu_{c1} = 0.1 \text{eV}$  and  $\mu_{c2} = 0.3 \text{eV}$ . It is illustrated in Fig. 4 that for the non-uniform biased sheets are able to turn the

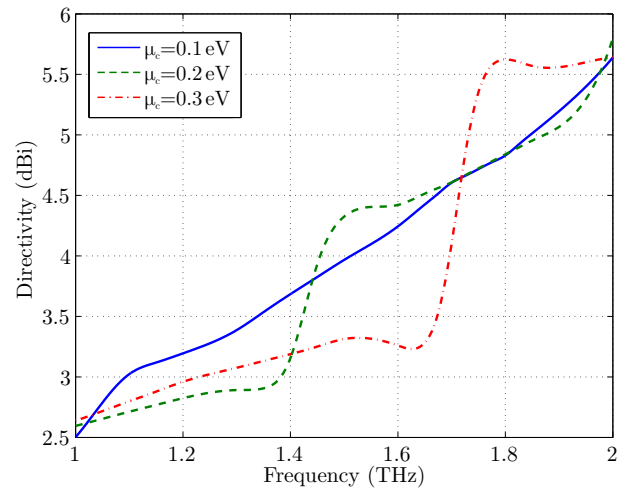


Fig. 3. Radar cross-section of a single graphene patch at a plane normal to plane wave direction and polarization.

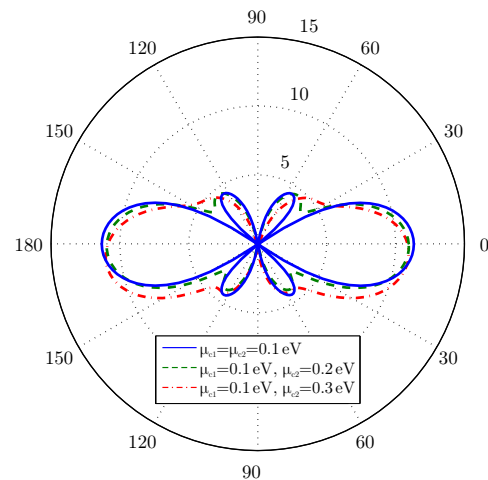


Fig. 4. Radar cross-section of a  $2 \times 2$  graphene patch array at  $xz$ -plane that is normal to plane wave direction and polarization.

main lobe. Specifically, the rotation angle is negligible for  $\mu_{c2} = 0.2 \text{eV}$ , since the directivity of the patches is almost identical. However, the main lobe turns considerably, about  $8^\circ$  for  $\mu_{c2} = 0.3 \text{eV}$  because of the increased directivity difference between the neighboring patches.

#### REFERENCES

- [1] L. Zhang, S. Mei, K. Huang, and C.-W. Qiu, "Advances in full control of electromagnetic waves with metasurfaces," *Advanced Optical Materials*, vol. 4, no. 6, pp. 818–833, 2016.
- [2] A. K. Geim and K. S. Novoselov, "The rise of graphene," in *Nanoscience and Technology: A Collection of Reviews from Nature Journals*. World Scientific, 2010, pp. 11–19.
- [3] G. D. Bouzianas, N. V. Kantartzis, T. V. Yioultis, and T. D. Tsioukakis, "Consistent study of graphene structures through the direct incorporation of surface conductivity," *IEEE Transactions on Magnetics*, vol. 50, no. 2, pp. 161–164, 2014.
- [4] V. Gusynin, S. Sharapov, and J. Carbotte, "Magneto-optical conductivity in graphene," *Journal of Physics: Condensed Matter*, vol. 19, no. 2, p. 026222, 2006.
- [5] G. W. Hanson, "Dyadic Green's functions and guided surface waves for a surface conductivity model of graphene," *J. Appl. Phys.*, vol. 103, no. 6, pp. 064302(1–8), 2008.